Nuclear Instruments and Methods in Physics Research A ▮ (▮▮▮▮) ▮▮▮–▮▮▮

Contents lists available at ScienceDirect

Nuclear Instruments and Methods in Physics Research A

journal homepage: www.elsevier.com/locate/nima

# Digital pulse shape analysis for the capture-gated liquid scintillator BC-523A

Marek Flaska *, Sara A. Pozzi

*Department of Nuclear Engineering & Radiological Sciences, University of Michigan, 1906 Cooley Building, 2355 Bonisteel Boulevard, Ann Arbor, MI 48109-2104, USA*

ARTICLE INFO

*Article history:*
Received 23 June 2008
Received in revised form
15 October 2008
Accepted 17 October 2008

*Keywords:*
Capture-gated detector
Liquid scintillator
Neutron spectroscopy
Special nuclear material

ABSTRACT

The BC-523A detector is a boron-10-loaded liquid scintillation detector that is sensitive to not only fast neutrons and gamma rays, but also to thermal neutrons. This detector has recently attracted the attention of several researchers and has shown promise for neutron spectroscopy. Several efforts have been made to accurately characterize this detector for several neutron and gamma-ray energies. In this paper, we show, for the first time, that neutron capture pulses can be visually distinguished from neutron scattering pulses by using an offline digital pulse shape discrimination method based on charge integration. In addition, new Monte Carlo simulation and measurement results for time to capture are compared and reasonable agreement is achieved. This work has applications in fields such as nuclear safeguards, nuclear nonproliferation, and national security.



## 1. Introduction

Accurate knowledge of neutron energy spectra is required in many areas; examples are nuclear nonproliferation, international safeguards, and national security. In particular, for nuclear nonproliferation, fast and robust methods for the identification special nuclear material (SNM) are needed. The identification of SNM with capture-gated organic liquid scintillators using fast digital techniques is a very promising method and is based on the neutron spectroscopic information that is available from the detector. The capture-gated organic scintillation detectors are very promising for all applications that require detailed neutron energy information; therefore, these detectors have potential to become one of the standard tools for neutron spectroscopy applications in mixed neutron–gamma-ray radiation environments.

Standard liquid scintillation detectors have been used as neutron detectors for many years, as a consequence of their excellent pulse shape discrimination (PSD) and timing properties. The capture-gated detectors are based on organic scintillators (liquid or plastic) that are loaded with material with high neutron absorption cross section. These materials are typically $^{10}$B, $^{6}$Li, and $^{nat}$Gd. The detectors can be used as full-energy neutron spectrometers and operated in the double pulse, or *capture-gated* mode [1].

The capture-gated detectors have been studied extensively in the past [2–7]. The neutron detection in these detectors relies on the measurement of two signals given by the same neutron colliding in a scintillation detector. Initially, the neutron interacts with hydrogen and carbon nuclei present in the active volume of the scintillation detector, thereby generating a typical scintillation pulse. Once the neutron has lost most of its energy, it has a high probability of being captured in the neutron-absorbing medium. Thus, a single neutron creates two pulses that are related in time. The primary (scattering) neutron pulse from the scintillator is accepted as the 'true' neutron pulse only if the subsequent (capture) neutron pulse is detected. This technique is referred to as *capture-gated neutron spectroscopy*. The prompt pulse amplitude is strongly correlated to the incident neutron energy, and this fact can be used to estimate the incident neutron energy. The elapsed time between the neutron scattering pulse and the subsequent neutron capture is typically of the order of several hundreds of nanoseconds.

In this work, we present new experimental results obtained with the BC-523A detector, a boron-loaded (4.41 wt% of $^{10}$B) liquid scintillator by Gobain [8], together with comparisons with Monte Carlo simulations. Recent studies (see, for example, [9]) have characterized this type of detector for different neutron sources. Other works have suggested the use of arrays of capture-gated neutron scintillators in instruments for nuclear materials characterization, such as multiplicity counters [10,11]. In addition, the paper by Swiderski et al. [12] presents a detailed comparison between BC-523A and BC-501A (standard Saint Gobain liquid scintillator) and concludes that the BC-523A detector in combination with a PSD zero-crossing method exhibits good resolving power for thermal neutrons.

The main objective of the present work was to develop an algorithm for the separation of capture pulses from scattering

*Corresponding author. Tel.: +1 734 764 0150; fax: +1 734 763 4540.
*E-mail addresses:* mflaska@umich.edu (M. Flaska), pozzisa@umich.edu (S.A. Pozzi).

0168-9002/$ - see front matter © 2008 Elsevier B.V. All rights reserved.
doi:10.1016/j.nima.2008.10.030

pulses measured by the detector. For the first time, it is shown that neutron capture pulses can be visually distinguished from neutron scattering pulses by using an offline digital PSD method.

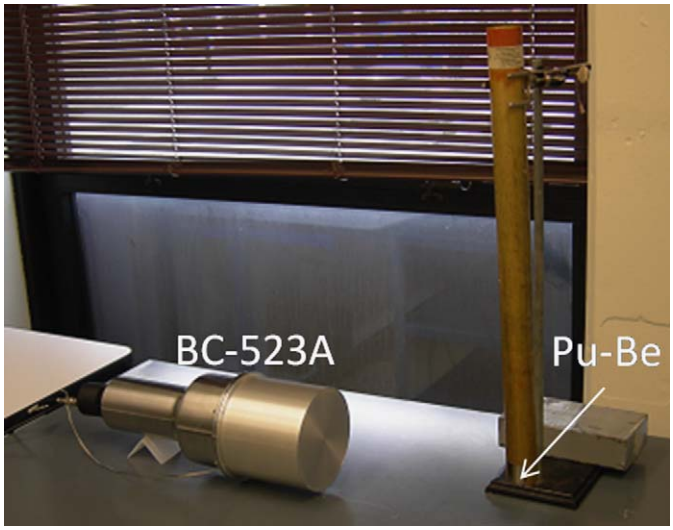


**Fig. 1.** Photograph of the BC-523A detector with the Pu–Be source.

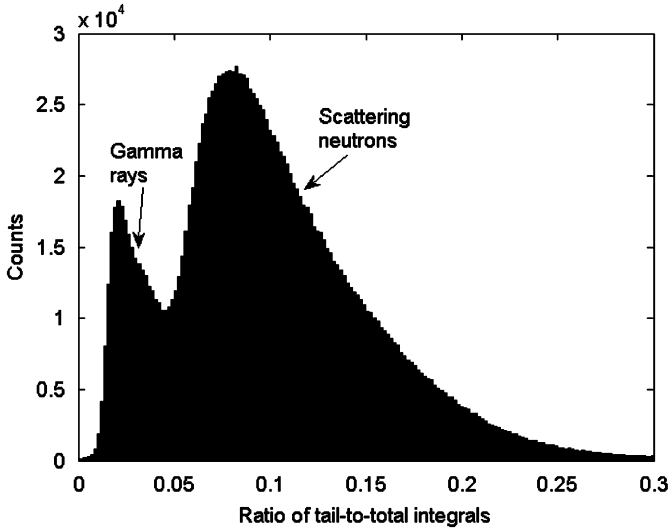


**Fig. 2.** Number of counts as a function of ratio of tail-to-total integrals. Gamma-ray pulses can be easily distinguished from fast neutron pulses. The long tail at high ratios of tail-to-total integrals is created by neutrons captured on $^{10}$B.

Another objective of this work was to verify the accuracy of Monte Carlo simulations by means of experimental results, and to reveal the details for the physical processes taking place in BC-523A. The simulations were performed with the Monte Carlo code MCNP-PoliMi [13]. The measurements were performed with BC-523A in conjunction with a Pu–Be source.

## 2. BC-523A measurements

In the initial measurements, a 1-Ci Pu–Be source was placed 30 cm from the face of the detector, as shown in Fig. 1. The source was located at the end of the manipulation rod. To increase the relative number of measured neutrons, a 2-in. lead shielding block (not shown in Fig. 1) was placed near the detector face. A 12-bit ADC250 waveform digitizer was used to collect several hundreds of thousand neutron and gamma-ray pulses. The digitizer operated at 250 MHz (4 ns sampling step) and each recorded waveform contained 60 steps (240 ns). The digitizer's internal threshold was set to 30 keVee (keV electron equivalent). An optimized PSD method [14] based on standard charge integration was applied to each measured waveform. Specifically, a ratio of tail-to-total-integrals was calculated for each pulse to distinguish gamma rays from fast and thermal neutrons. In liquid scintillators, neutrons generally create pulses with larger tails than gamma rays; this fact is employed in the ratio calculation [1]. In plastic scintillators, this approach is limited by performance of scintillation materials and photomultipliers [15]. The tail integration started 56 ns and ended 180 ns from the pulse maximum. The total integral was calculated from the beginning of the pulse to 180 ns after the pulse maximum. The integration intervals were selected by optimizing the PSD method with the objective of minimizing the number of misclassified pulses.

Fig. 2 shows a typical PSD distribution that shows the number of counts as a function of the pulse integral ratios. Specifically, the data is shown as a histogram that contains all accepted pulses. Scattering neutrons and gamma rays can be distinguished in Fig. 2, similar to standard liquid scintillators. The relatively large overlap area is due to the very low measurement threshold, which brings uncertainty to the PSD [16].

Fig. 3 shows the neutron capture events more explicitly. For the first time, the neutron capture pulses and the neutron and gamma-ray scattering pulses measured with BC-523A are unambiguously identified. The identification is possible because the neutron capture reaction on $^{10}$B-10 generates a recoil alpha particle, which generates a pulse having a more pronounced tail than either neutron or gamma-ray scattering pulses. This consideration is verified in the distributions shown in Fig. 3(a),

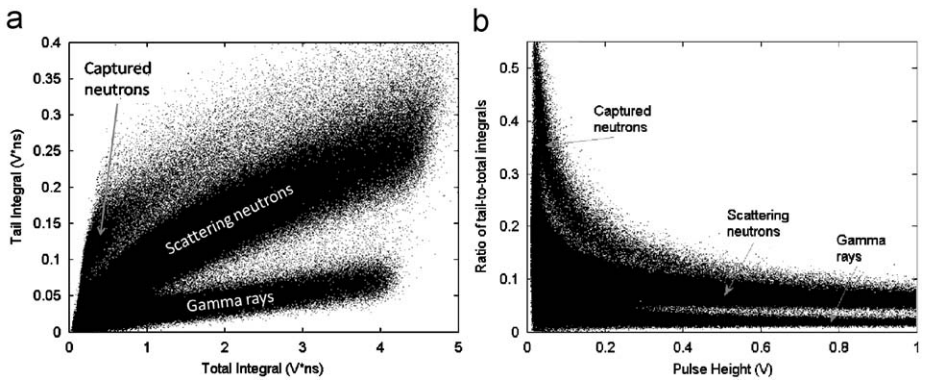


**Fig. 3.** Tail integral versus total integral (a). Gamma-ray pulses can be distinguished not only from fast (scattering) neutron pulses, but also from thermal (capture) neutron pulses. Ratio of tail-to-total integrals versus pulse height (b). Three regions of pulses are clearly distinguished.

Please cite this article as: M. Flaska, S.A. Pozzi, Nucl. Instr. and Meth. A (2008), doi:10.1016/j.nima.2008.10.030

where the pulse tail integral is shown as a function of total integral, and in Fig. 3(b), where the ratio of tail-to-total integrals is shown as a function of pulse height. There are a total of $\sim 1.7e^6$ pulses shown in Fig. 3. As expected, the capture pulses are observed at high ratio values, thus above the neutron and gamma-ray scattering pulses. To see the three regions of pulses more clearly, a smaller number of pulses is shown in Fig. 4 ($\sim 6e^5$ pulses in total). In addition, for clarity smaller scales were chosen in Fig. 4. Approximately 1.6% of the measured pulses are identified as capture pulses. The ratio of capture and neutron scattering pulses is approximately 2.3%.

It should be noted that the capture events cannot be directly seen in the histogram in Fig. 2, because the ratio values of the capture pulses are spread over a large range. Moreover, the total number of capture pulses is low compared to scattering pulses. Typical pulses obtained from the BC-523A are shown in Fig. 5.

To verify the observation of three regions of pulses and their good separation, the BC-523A detector was surrounded by 1 in. of polyethylene (PE). In addition, the Pu–Be source was placed inside the borated PE storage barrel, as shown in Fig. 6. One of the barrel ports was opened to allow the source particles to reach the detector. The 2-in. Pb shielding was used between the open port of the source barrel and the detector. The PE shielding around the detector was used to increase the number of captured neutrons by backscattering the neutrons leaving the detector. Indeed, the number of captured neutrons identified by the PSD method increased by 12% in the presence of PE when compared to the case without the PE. These captured neutrons were located in the area of low total integrals and high tail integrals shown in Figs. 3(a) and 4.

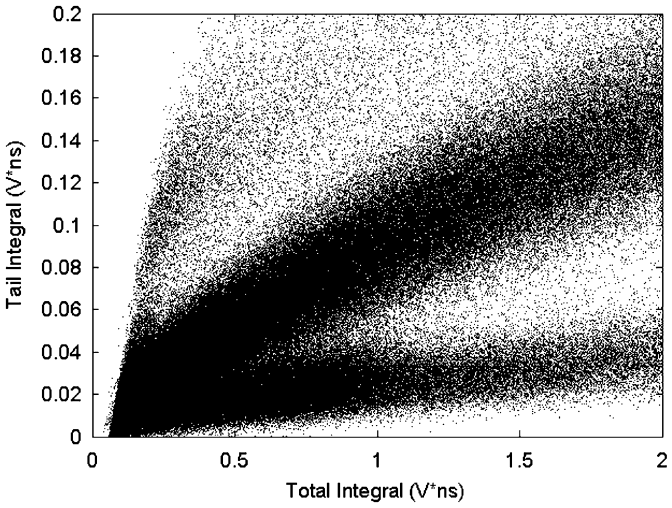


**Fig. 4.** Tail integral versus total integral. Very good separation of captured neutrons from scattering neutrons and gamma rays.

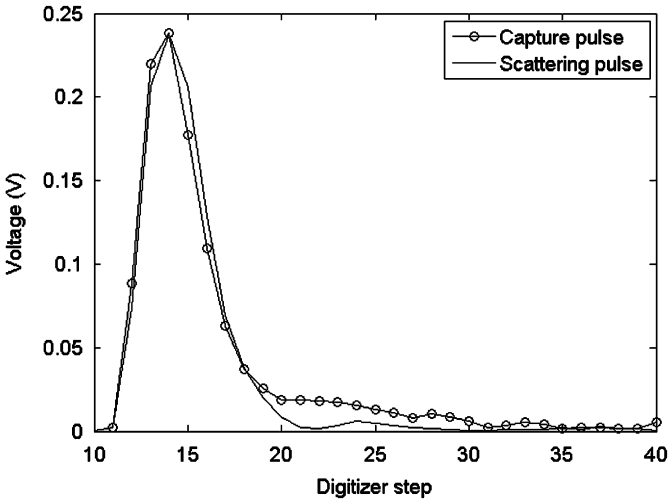


**Fig. 5.** Example of neutron capture and neutron scattering pulses measured with the BC-523A detector.

## 3. Monte Carlo simulations

Several simulations were performed by using the MCNP-PoliMi code to reveal the details of the physical processes that take place in the BC-523A detector. The MCNP-PoliMi code was developed to provide accurate information, on event-by-event basis, on neutron and gamma-ray time quantities. The code computes many quantities of interest, such as the type, position, and time of each collision, the particle energy prior to collision, as well as the remaining energy, and neutron and gamma-ray pulse height distributions. Subsequently, the postprocessors specially designed to extract the relevant information from the simulations provide quantities such as the detector efficiency, the number of scattering events undergone by the neutron prior to capture, the energy prior to capture, the time to capture, etc.

The MCNP-PoliMi simulation results presented here were obtained for a detailed BC-523A detector model. The active part of the detector is 13 cm high, with a diameter of 12.6 cm. Cf-252, Pu–Be (high-purity Pu-239), and several monoenergetic, isotropic gamma-ray and neutron sources were used in conjunction with the detector, each at a distance of 30 cm from the detector.

Figs. 7(a) and (b) show the number of neutron elastic and capture collisions for the Cf-252 and Pu–Be for varying depth of the active cell of the detector. The distributions are similar in the two cases, although the average neutron energy of the Pu–Be source causes the maximum number of counts to be reached deeper in the detector than in the case of Cf-252. In both cases, the maximum is reached at lower depths for elastic scatterings than for captures. This result is expected because the sources have different neutron spectra and their neutrons typically need to lose most of the energy prior to capture.

Fig. 8 (a) shows the number of gamma-ray Compton-scattering collisions for the Cf-252 source for varying depth of the active cell of the detector. Compton scattering is the most probable collision gamma rays undergo in the detector. It can be seen in Fig. 8(a) that the maximum is reached at a much lower depth in the detector (a few mm) when compared to the neutron collisions. After reaching the maximum the number of collisions decreases and reaches 50% of the maximum value at a depth of approximately 10 cm.

Fig. 8(b) shows the neutron fluence for the Pu–Be source along the center plane ($xy$ plane, $z$=0 cm) of the detector. As expected, the neutron fluence decreases with increasing depth. Also, the highest fluence is reached at position close to $x$=$y$=$z$=0 cm. In Fig. 8(b), a step of 2.5 mm was used.

## 4. Comparison measurements versus simulations

The measured pulses were analyzed with an algorithm that extracts the neutron capture pulses on the basis of the calculated ratio. Then, the primary neutron scattering pulses were identified by applying the PSD method to the pulses that preceded the capture pulses. If the preceding pulse that was accepted was identified as a scattering neutron pulse, this pulse was considered a non-accidental (confirmed) neutron pulse. These neutron pulses

Please cite this article as: M. Flaska, S.A. Pozzi, Nucl. Instr. and Meth. A (2008), doi:10.1016/j.nima.2008.10.030

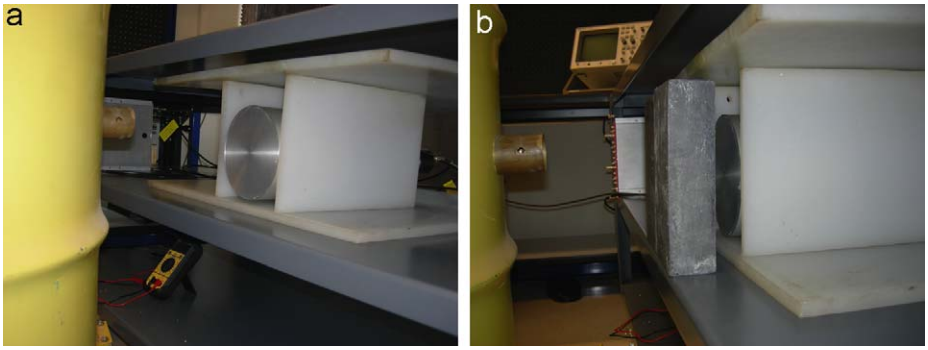


**Fig. 6.** Photographs of the BC-523A detector and the Pu–Be source inside the storage barrel. The detector was surrounded by 1 in. of polyethylene (a) and shielded by 2 in. of lead (b). Two separate shielding configurations are shown to allow the reader to see all parts of the experimental setup.

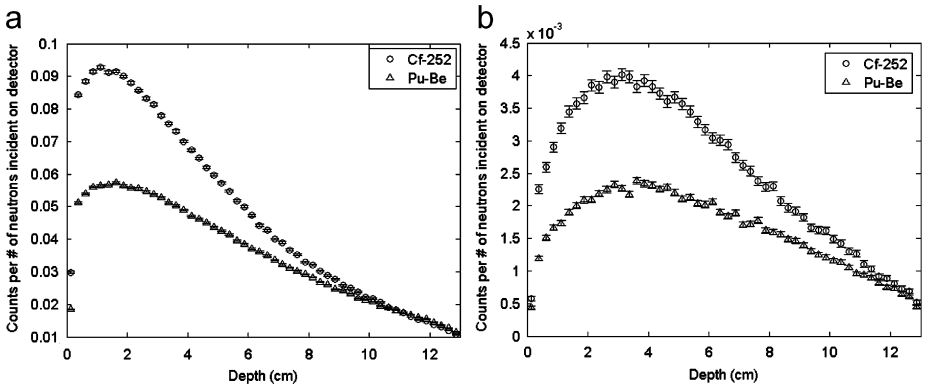


**Fig. 7.** Number of neutron elastic (a) and capture (b) collisions as a function of the detector depth. Maxima are reached below 2 cm for elastic collisions and below 4 cm for capture collisions. Error bars show $1\sigma$ statistical uncertainties.

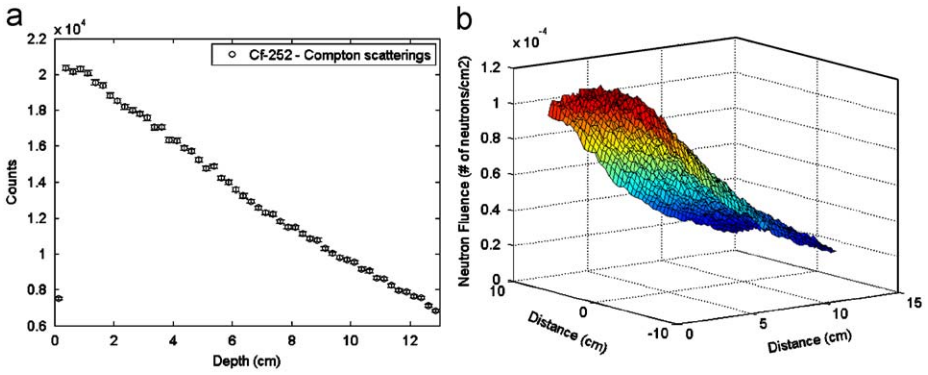


**Fig. 8.** (a) Number of Compton scatterings for Cf-252 as a function of the detector depth. Maximum is reached below 0.5 cm. $1\sigma$ statistical uncertainties are shown. (b) Neutron fluence for Pu–Be in BC-523A on the $xy$ plane, $z$=0 cm (right). Maximum is reached close to $x$=$y$=$z$=0 cm. No statistical uncertainties are shown.

were then used to build pulse height distributions for subsequent analysis and comparisons with the simulations.

For the simulation data, the neutron energy depositions in the detector were converted to light output. This conversion was performed using the calibration curves of the standard liquid scintillator [17] because of the lack of calibration data for BC-523A. Fig. 9(a) shows the comparison of measured and simulated neutron pulse height distributions. A relatively good agreement was obtained between the simulation and the measurement. Two possible explanations for the observed differences between simulation and measurement are the approximate energy-to-light conversion described above and the particle classification error (PSD error).

Fig. 9(b) shows the comparison between measured and simulated time-to-capture distributions. The data were normalized to area to allow for the comparison and relatively good agreement is obtained. The observed difference is probably caused primarily by the PSD error.

Both measurement and simulation results were obtained for times between initial neutron scattering pulses and subsequent capture pulses. The average times are approximately 703 and 973 ns for the simulation and the measurement, respectively. The observed time difference is caused mostly by the PSD misclassification, especially at low energies, as shown in Fig. 2 (overlap area between scattering neutrons and gamma rays). In addition, some minor effect is expected from omitting walls in the

Please cite this article as: M. Flaska, S.A. Pozzi, Nucl. Instr. and Meth. A (2008), doi:10.1016/j.nima.2008.10.030

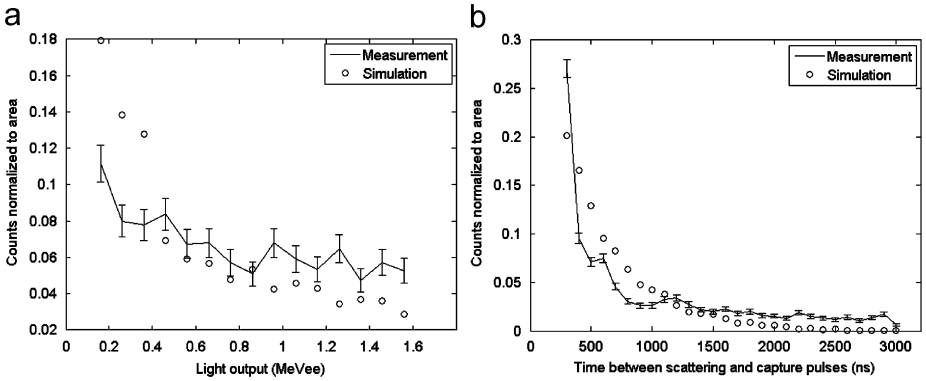


**Fig. 9.** Measured and simulated neutron (a) pulse height distributions and (b) time-to-capture distributions. $1\sigma$ statistical uncertainties are shown for the measurement data.

simulation to simplify the geometry (neutron backscattering effect not simulated).

The official Saint Gobain documentation estimates the average time value to ~500 ns. This value is in very good agreement with the value of 490 ns found in literature [7]. Both simulation and measurement time values obtained in the present study are larger than this reported value because of the size of the data acquisition window used. This time window introduces the system dead time; consequently, the capture pulses arriving at the detector within this window cannot be detected. It should be noted that the time-to-capture value was accepted only if it was lower than 3 μs. This value was chosen based on the simulation results that indicated that after 3 μs the fraction of correlated neutron capture events is negligible when compared to the number of accidentals.

## 5. Conclusions

In this paper, for the first time, a method is presented to visually distinguish neutron capture pulses from neutron scattering pulses measured with the BC-523A detector. This new capability is very important for neutron spectroscopy with this type of detector, which is very promising for use in applications aimed at detection of special nuclear material (SNM) and radioactive sources. Because this detector is sensitive not only to fast neutrons and gamma rays, but also to thermal neutrons, this detector is a very good candidate for neutron spectroscopy applications. Monte Carlo simulations were carried out to characterize the time to neutron capture in the detector, and good agreement was obtained with the measurements. The use of capture-gated organic scintillation detectors shows promise in the area of the detection of SNM because these detectors can be built reasonably small for hand-held devices, while still being efficient. In fact, detection systems based on the measurement of both neutrons and gamma rays are less vulnerable to false alarms, especially in the presence of shielding. Future work includes the evaluation of the detection efficiency for typical neutron sources measured with and without shielding, and neutron spectrum unfolding.

## Acknowledgments

The authors would like to thank to Dr. Schillebeeckx from EC-JRC-IRMM in Geel, Belgium for providing the BC-523A detector, and Dr. Ulbricht from ULTRONICS Instrument Co., Richland, Washington (ultronicsinstruments@yahoo.com) for providing the ADC250 waveform digitizer and the data acquisition software.

## References

[1] G.F. Knoll, Radiation Detection and Measurement, third ed, Wiley, New York, 2000, pp. 570.
[2] D.M. Drake, W.C. Feldman, C. Hurlbut, Nucl. Instr. and Meth. A 247 (1986) 576.
[3] H.P. Chou, C.Y. Horng, Nucl. Instr. and Meth. A 328 (1993) 522.
[4] B. Czirr, G. Jensen, Nucl. Instr. and Meth. A 349 (1994) 532.
[5] B. Czirr, D. Merrill, D. Buehler, Nucl. Instr. and Meth. A 476 (2002) 309.
[6] S. Normand, B. Mouanda, S. Haan, M. Louvel, IEEE Trans. Nucl. Sci. NS-49 (2002) 577.
[7] S.D. Jastaniah, P.J. Sellin, Nucl. Instr. and Meth. A 517 (2004) 202.
[8] Saint-Gobain Crystals and Detectors, BC-523A Product Data Sheet, 〈http://www.detectors.saint-gobain.com/Media/Documents/S000000000000000001004/SGC_BC523A_Data_Sheet.pdf〉.
[9] T. Aoyama, K. Honda, C. Mori, K. Kudo, N. Takeda, Nucl. Instr. and Meth. A 333 (1993) 492.
[10] A.P. Belian, et al., Nucl. Instr. and Meth. A, 505 (2003) 54.
[11] M.C. Miller, Neutron detection and multiplicity counting using a boron-loaded plastic scintillator/bismuth germanate phoswich detector array, LA-13315-T, Los Alamos National Laboratory, 1997.
[12] L. Swiderski, et al., Boron-10 loaded BC523A liquid scintillator for neutron detection in the border monitoring, in: Proceedings of the Nuclear Science Symposium and Medical Imaging, IEEE conference, Honolulu, Hawaii, USA, October 27–November 3, 2007.
[13] S.A. Pozzi, E. Padovani, M. Marseguerra, Nucl. Instr. and Meth. A 513 (2003) 550.
[14] M. Flaska, S.A. Pozzi, Nucl. Instr. and Meth. A 577 (2007) 654.
[15] P.L. Reeder, A.J. Peurrung, R.R. Hansen, D.C. Stromswold, W.K. Hensley, C.W. Hubbard, Nucl. Instr. and Meth. A 422 (1999) 84.
[16] R. Aryaeinejad, E.L. Reber, D.F. Spencer, IEEE Trans. Nucl. Sci. NS-49 (2002) 1909.
[17] S.A. Pozzi, J.A. Mullens, J.T. Mihalczo, Nucl. Instr. and Meth. A 524 (2004) 92.

Please cite this article as: M. Flaska, S.A. Pozzi, Nucl. Instr. and Meth. A (2008), doi:10.1016/j.nima.2008.10.030